http://dx.doi.org/10.5012/bkcs.2012.33.8.2635

Preparation and Investigation on Swelling and Drug Delivery Properties of a Novel Silver/Salep-g-Poly(Acrylic Acid) Nanocomposite Hydrogel

Ghasem Rezanejade Bardajee,* Zari Hooshyar, and Firozeh Kabiri

*Department of Chemistry, Payame Noor University, PO Box 19395-3697, Tehran, Iran. *E-mail: rezanejad@pnu.ac.ir*
Received March 19, 2012, Accepted May 9, 2012

Novel silver/salep-g-poly(acrylic acid) nanocomposite hydrogel were prepared in aqueous solution using poly(acrylic acid) grafted onto salep as a biopolymer based material. FT-IR spectra confirmed that poly(acrylic acid) (PAA) had been grafted onto salep in graft copolymerization reaction. TEM observations showed that silver nanoparticles have been uniformly dispersed in polymeric matrix. Effects of pH, acrylic acid (AA) amount and silver ion concentration on swelling capabilities were investigated. Results indicate that modifying AA and silver ion can improve swelling properties of the resultant nanocomposite hydrogel. pH response of this nanocomposite hydrogel in acidic and neutral pH made it suitable for drug delivery applications.

Key Words : Nanocomposite hydrogel, Silver, Salep, Swelling, Drug delivery

Introduction

Hydrogel nanocomposites (HNs), which includes the incorporation of inorganic nanoparticles inside three-dimensional polymeric networks, have been attracted great interests in recent years because of their intrinsic advantages over pure hydrogels or inorganic nanoparticles.[1-4] Recently, silver nanoparticles have been widely utilized in hydrogels field due to remarkably improvement some properties of hydrogel such as mechanical toughness, large deformability, high swelling/deswelling rates, excellent electrical conductivity, antimicrobical effects, and optical properties, and high transparency.[5-7] It has been found that high efficiency of silver HNs extremely correlate on the size of the nanoparticles in hydrogel which should be as small as possible with a narrow size distribution. On the other hand, silver should be well dispersed on the surface of the hydrogels without the formation of large aggregates, which otherwise dramatically reduce the properties of silver.[8-11] To improve the dispersion of nanoparticles inside the hydrogel matrix, and also partially prevent the formation of aggregates, the entrapment of silver cations by hydrogel matrix followed by reduction with common reducing agents has been preferred to the simple mixing of the two components and the polymerization in the presence of pre-synthesized silver nanoparticles.[12-16] However, the reducing agents are toxic reagents and the synthesis conditions are harsh that may limit the potential of silver HNs for biomedical applications. From that viewpoint and taking into account the fact that the application of silver nanocomposites are mostly toward biomedical treatment, use of biopolymer- based hydrogels and nontoxic reagents have definitely emerged as strong challenges in this field.

In this work, we introduce an easy way to synthesis a silver HN without using any extra reducing agent at room temperature. The hydrogel networks were prepared by graft copolymerization of poly(acrylic acid) onto salep (salep-g-PAA) in water. The structure of HN and the influences of silver content and monomer concentration on the swelling behavior of HN were studied. In addition, due to the applications of the salep-g-PAA in drug delivery, the release profile of the prepared silver/salep-g-PAA was studied using diclofenac sodium (DS) as a model drug.

Experimental

Materials. Salep was purchased from a supplier in Kordestan, Iran ($M_n = 1.17 \times 10^6$ g/ mol, $M_w = 1.64 \times 10^6$ g/ mol (high M_w), PDI = 1.39, eluent = water, flow rate = 1 mL/ min, acquisition interval = 0.43 s from GPC results). Silver nitrate ($AgNO_3$, from Fluka, St. Louis, MO), methylenebisacrylamide (MBA, from Merck, Darmstadt, Germany) as a crosslinker, ammonium persulfate (APS, from Fluka, St. Louis, MO) as a water soluble initiator, and acrylic acid (AA, from Merck) as a monomer, were analytical grades and used without further purification. Diclofenac sodium (DS) was received from Alborz Darou Co., Tehran, Iran as a gift. All other chemicals were also analytical grade. In through experiment, double distilled water (DDW) was used for preparing solutions. For preparation of HNs, sunlight-UV in winter was used.

Instrumental Analysis. FT-IR spectra of samples in the form of KBr pellets were recorded using a Jasco 4200 FT-IR spectrophotometer. A Shimadzu UV-visible 1650 PC spectrophotometer was used for recording absorption spectra in solution. All samples were placed in a 1.00 cm quartz cuvette for UV measurements. The dynamic weight loss tests were conducted on a TA instrument 2050 thermo-gravimetric analyzer (TG). All tests were conducted under N_2 atmosphere (25 mL/min) using sample weights of 5-10 mg over a temperature range of 25-700 °C at a scan rate of 20 °C/min. The mass of the sample pan was continuously recorded as a function of temperature. The morphology of the dried samples was examined using a scanning electron microscope (SEM)

(Philips, XL30) operated at 10 kV after coating the dried samples with gold films. Transmission electron microscopy (TEM) was taken on a Zeiss TEM at an acceleration voltage of 80 kV. Samples for TEM were prepared by putting a drop of solution on a carbon-coated copper grid.

Preparation of Silver/Salep-g-PAA HNs. In general, salep (1.0 g) was added to H_2O (80 mL) at a three-neck reactor equipped with a mechanical stirrer while stirring (200 rpm). After homogenization, 5 mL of the different concentrations of $AgNO_3$ (0.00, 0.002, 0.005, 0.01 and 0.05 mol/L) was added to the reaction mixture and it was stirred for further 30 min. The reactor was placed in a thermostated water bath (80 °C) and 5 mL of the AA monomer solution (0.06, 0.12, 0.18, 0.24 mol/L), 5 mL of the MBA crosslinker solution (6.5×10^{-3} mol/L), and 5 mL of APS initiator solution (1.65×10^{-2} mol/L) were added and the reaction mixture was stirred until a gel-like product was observed after around 20 min. Finally, the reaction mixture was cooled to room temperature and the product was poured into 100 mL of ethanol, remained for 2 h and then chopped to small pieces for further drying. To remove the sol fraction of mixture (uncrosslinked and not grafted PAA, uncrosslinked salep and possibly also some unreacted monomer), the dewatered hydrogel was allowed to completely swell for overnight in plenty of distilled water (400 mL) and then dewatered in ethanol (200 mL, 2 h). The non-solvent ethanol was decanted and then 100 mL fresh ethanol was added. The chopped particles were further remained for 24 h in ethanol to completely dewater. The dewatered gel particles were filtered and dried in oven (at 50 °C) for 24 h. After grinding, the powdered HNs were stored in the absence of moisture, heat, and light for further experiments.

Swelling Measurement. Dried silver/salep-g-PAA HN of known weights were put in tea bag (*i.e.*, a 100 mesh nylon screen) and immersed in 100 mL of DDW or solutions with different pHs at 37 °C. All of the buffered solutions were prepared according to Merck Co. procedure. The pH 2 was prepared by adding KCl (0.2 M, 50 mL) and HCl (0.2 M, 13 mL) solution in a 200 mL volumetric flask and then the water was added to volume. The pH 4 was prepared by adding potassium biphthalate (0.2 M, 50 mL) and HCl (0.2 M, 0.1 mL) solution in a 200 mL volumetric flask and the water was added to volume. The pH 6 was prepared by adding monobasic potassium phosphate (0.2 M, 50 mL) and NaOH (0.2 M, 5.6 mL) solution in a 200 mL volumetric flask and the water was added to volume. The pH 8 was prepared by adding boric acide and KCl (0.2 M, 50 mL) and NaOH (0.2 M, 3.9 mL) solution in a 200 mL volumetric flask and the water was added to volume. The pH 10 was prepared by adding boric acide and KCl (0.2 M, 50 mL) and NaOH (0.2 M, 43.7 mL) solution in a 200 mL volumetric flask and the water was added to volume. In order to more ensure, the pH of all buffer solutions were also measured by pH meter. In order to eliminate the effect of salt on the swelling of hydrogels, the ionic strength of the all buffer solutions was fixed on 9.5 mS/cm by KCl solution. After that, the pH of all buffer solutions was measured again by pH meter. The tea bag was hung up for 5 min in order to remove the excess solution. The swelling was calculated according to following equation (Eq. 1) and reported as grams of water per grams of resin (g/g).

$$\text{Swelling (g/g)} = \frac{\text{Weight of swollen gel}}{\text{Weight of dried gel}} - 1 \qquad (1)$$

Drug Loading and Releasing. DS loading in the silver/salep-g-PAA HN was performed by diffusion method. 0.1 g of powdered silver/salep-g-PAA HN was added in tea bag (*i.e.*, a 100 mesh nylon screen) and was immersed entirely in 60 mL of DS solution (0.1 mol/L, W_a) for 2 hours to complete drug loading. Then, the amount of DS in solution (W_b) was determined by UV-vis spectroscopy at characteristic λ_{max} (278 nm). After loading, the content of tea bag was removed and washed by 10 mL DDW to remove DS existing on the surface of silver/salep-g-PAA HN (W_c). The DS loading efficiency was calculated as follows (Eq. 2):

$$\text{DS loading efficiency (\%)} = \left(\frac{W_a - W_b - W_c}{W_a}\right) \times 100 \qquad (2)$$

The DS loading efficiency was estimated 84.2% after 2 hours.

The release rate experiments were performed in buffered solutions at 37 °C under unstirred conditions. The DS loaded silver/salep-g-PAA HN was put in a 100 mL beaker containing buffered solutions. At a given time intervals, 1 mL of filtered samples were withdrawn and assayed for the amount of released drug to the solution. The amount of released drug was determined by UV spectroscopy at characteristic λ_{max} using a calibration curve constructed from a series of drug solutions with known concentrations.

Results and Discussions

Mechanism of Silver/Salep-g-PAA HN Formation. For preparation of silver/salep-g-PAA HNs, sunlight-UV as a gratis source of reducing agent, and salep as a biocompatible, biodegradable, non-toxic, effective capping agent, and multifunctional material was utilized to inhibit the agglomeration of the freshly prepared silver nanoparticles in solution.[17-19] In this approach, the coordinated silver cations were reduced into the silver nanoparticles by photochemical reactions. The schematic representation of this conversion was indicated in Scheme 1. In detail, *in-situ* reduction of silver ions and stabilization of particles can be explained by two steps. Firstly, metal ions are anchored by functional groups of salep backbones (hydroxyl groups of glucomannan repeating units), and metal reduction process takes place in the presence of sunlight UV-irradiation, to give salep capped silver nanoparticles. Secondly, ammonium persulfate, as an initiator, is decomposed under heating and produced sulfate anion-radicals that remove hydrogen from anomeric carbon or OH groups of salep backbones. This persulfate-saccharide redox system results in active centers capable to radically initiate polymerization of AA monomers and leading to a graft copolymer. Since the crosslinking agent, MBA, is

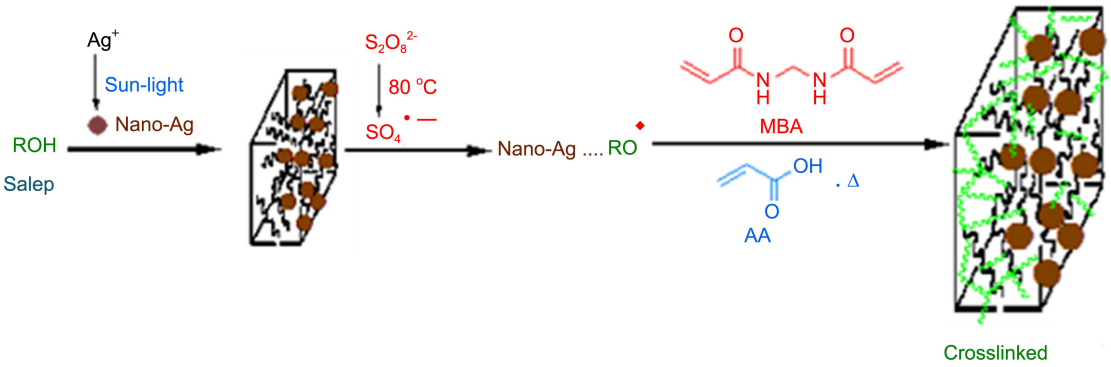

Scheme 1. Proposed mechanism pathway for the synthesis of silver/salep-g-PAA HN.

accessible in the system, the copolymer comprises a cross-linked nanocomposite structure. The hydrogel networks around nanoparticles effectively inhibit their aggregation for longer periods and can be extracted into water whenever they are required for usage.

Swelling Study. The effect of monomer concentration on water absorption of the silver/salep-g-PAA HNs was investigated by varying the AA concentration from 0.06 to 0.24 mol/L whereas the amount of $AgNO_3$ was kept at 0.01 mol/L. As shown in Figure 1, increasing the monomer concentration up to 0.12 mol/L, the swelling capacity is increasing initially and then it is considerably decreased with further increasing in monomer amount. The maximum absorption was obtained when the monomer concentration was 0.12 mol/L. The initial increase in water absorption can be explained by the fact that an increase in monomer concentration led to more grafting of AA onto salep. This led to better formation of polymer networks; consequently the water absorption is increased. The swelling decreases after the maximum can be attributed to increase in viscosity of the medium which hinders the movement of free radicals and monomer molecules.

Diffusion behavior of silver/salep-g-PAA HN regarding the amount of AA content was also analyzed by using following equation (Eq. 3):[20,21]

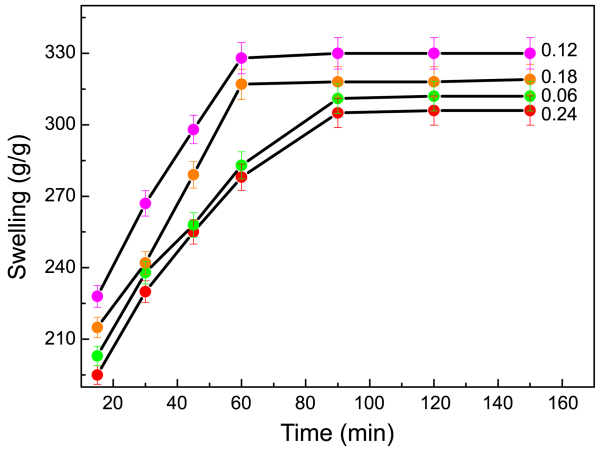

Figure 1. Effect of monomer concentration on swelling capacity of silver/salep-g-PAA HN ($AgNO_3$ = 0.01 mol/L) in DDW at 37 °C.

$$F = kt^n \quad (3)$$

here F is fractional uptake at time t and k is characteristic constant of hydrogel and n is characteristic exponent of the mode of transport of the penetrating molecule. The n and k values obtained from Figure 1 are given in Table 1. The value of n is responsible to show rate determining step of swelling mechanism. Three steps are considered to direct hydrogel swelling in water. First is the penetration of water into the hydrogel structure. Second is the loosening up of hydrated polymer chains and third is expansion of hydrogel structure into the surrounding water. The hydrophilic polymer's response towards water is depicted in three models. Depending on the value of n, different mechanism can be considered for swelling. For example, when n is bellow 0.45, the Fickian diffusion phenomenon dominates, and when n is between 0.45 and 0.89, an anomalous transport (non-Fickian diffusion), which often termed as first-order release, is dominated. After the n value reaches 0.89 and above, this can be characterized by case II and super case II transport, which means the rate does not change over time (zero order). It has seen that the transport model is Fickian in all examined AA amounts in silver/salep-g-PAA NH as shown in Figure 1.

To test the influence of the $AgNO_3$ concentration on the swelling capacity of the silver/salep-g-PAA HNs, we kept all other experimental variables constant and different amounts of $AgNO_3$ (0.00, 0.002, 0.005, 0.01 and 0.05 mol/L) were added to the reaction mixture (the monomer concentration was adjusted to 0.12 mol/L). Figure 2 shows the swelling capacity of the silver/salep-g-PAA HNs at various concentrations of $AgNO_3$ after 60 min at 37 °C. As one can see in Figure 2, with increasing the $AgNO_3$, the water absorbency of the hydrogel was decreased. This decreasing of the swell-

Table 1. Diffusion parameters of silver/salep-g-PAA HN samples at different monomer concentrations

AA concentration (mol/L)	R^2	n	log k
0.06	0.994	0.233	-0.420
0.12	0.993	0.258	-0.466
0.18	0.951	0.273	-0.502
0.24	0.997	0.253	-0.453

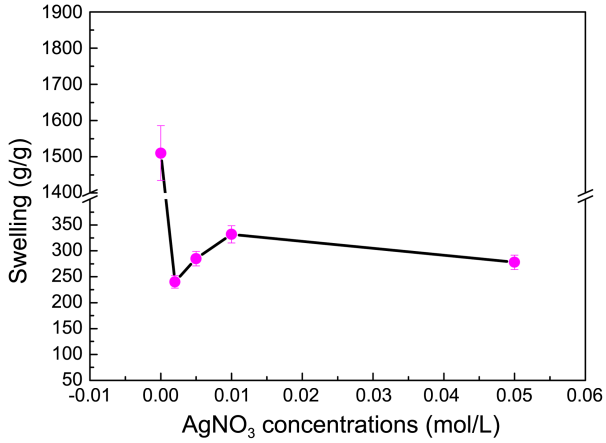

Figure 2. Effect of $AgNO_3$ content on swelling capacity of silver/salep-g-PAA HN (AA = 0.12 mol/L) in DDW after 60 min at 37 °C.

ing capacity value may be attributed to the chelation of some hydroxyl and carboxylate groups of the hydrogel networks with silver nanoparticles which neutralize the repulsions in the networks. In the remainder of this manuscript, the silver/salep-g-PAA HN with content of 0.12 mol/L AA and 0.01 mol/L $AgNO_3$ was chosen as the optimum sample and used for further investigations.

Presence of carboxylate groups of PAA in the HN allows supposing the possible pH-sensitivity of the synthesized silver/salep-g-PAA. In this regard, effect of pH on the swelling of silver/salep-g-PAA HN was investigated (Figure 3). As one can see in Figure 3, the swelling increases with rising pH up to 8 and then it decreases at pH = 10. It has been observed that maximum degree of swelling was observed at pH 8. The anion-anion repulsive forces between the groups (for example, carboxylate groups) in the networks of the hydrogel are the main reason for the swelling at pH 8. The high susceptibility of silver/salep-g-PAA HN to pH changes can be attributed to the presence of ionic groups from the ionization of AA part or salep part in the hydrogel. We believe that carboxyl groups are the major component responsible for the pH dependency of the system. The charge state of the system will change drastically above pK of COOH, and the swelling measurements in buffer solutions with pHs 2 and 4 proves this idea (Figure 3). In addition, the swelling should not theoretically decrease at pH 10 in our new conditions (different pHs with the same ionic strength), but the results in Figure 3 don't confirm this theory. In high basic solutions, the hydroxyl groups on the salep backbone can ionize to reactive alkoxy anions which subsequently can react with carboxylic acid (or corboxylate) groups of the hydrogel to make an ester moiety. This reaction can make more networks in the hydrogel which is responsible for the lower swelling of the hydrogel. This ester moiety formation can also decrease the hydrophilicity of the whole network. It is well known that swelling ability of ionically networks depends strongly on hydrophilicity of the whole network. The hydrogel after this reaction can become less hydrophilic as a result of loss of alkoxy and carboxylate anions.

The anion-anion repulsive forces between the groups (for example, carboxylate groups) in the networks of the hydrogel are the main reason for their swelling. As the pH decreases, swelling capacity of silver/salep-g-PAA HN also decreases. At low pH, the H^+ ions in the external medium effectively suppress the ionization of the AA or the OH of salep. This effectively decreases the concentration of mobile ions inside the silver/salep-g-PAA HN. This causes the decrease of osmotic pressure, which ultimately reduces the swelling capacity of silver/salep-g-PAA HN. On the other hand, the increase in pH facilitates the ionization of the groups, thus, there is an increase in anion-anion repulsive forces between the carboxylate groups which increases the swelling of the silver/salep-g-PAA HN (higher osmotic pressure between external medium and hydrogel networks). At high pH, the ion swelling pressure begins to drop again. Because of increase in ionic strength of the swelling medium, the ion osmotic swelling pressure decreases. In this regard, for having the higher swelling, we need higher basic condition than pK_a equilibrium to obtain more carboxylate anions in the hydrogel structure.

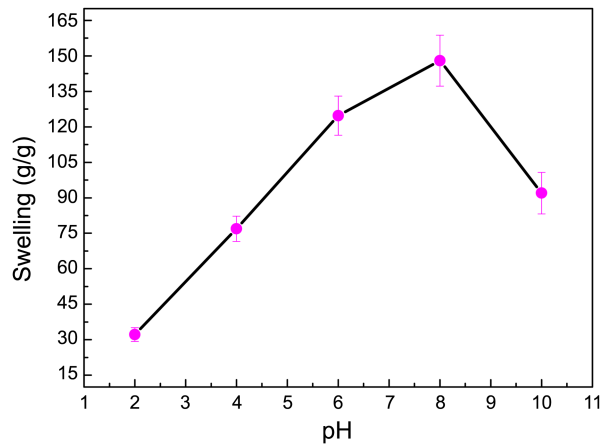

Figure 3. pH swelling dependency of the silver/salep-g-PAA HN after 60 min at 37 °C.

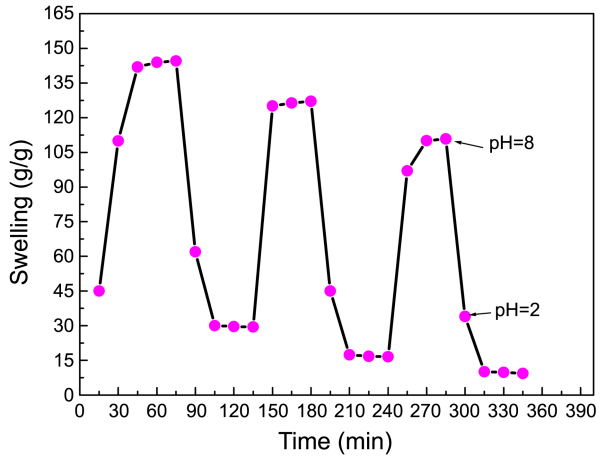

Figure 4. pH-reversibility of silver/salep-g-PAA HN with 60 min time intervals between the pH changes at 37 °C.

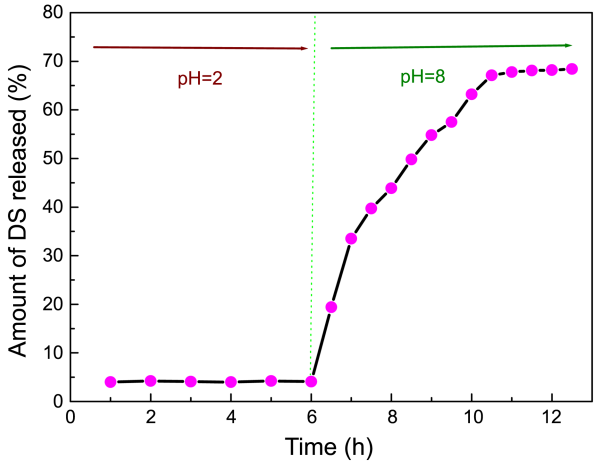

Figure 5. DS release profile of silver/salep-g-PAA HN at pH 2 and pH 8.

In continue, the reversible swelling-deswelling behavior of silver/salep-g-PAA HN in solutions with pH 2 and 8 was examined (Figure 4). At pH 8, the hydrogel swells due to anion-anion repulsive electrostatic forces, while at pH 2, it shrinks within a few minutes due to protonation of the carboxylate anions. This swelling-deswelling behavior of the hydrogel makes silver/salep-g-PAA HN as a suitable candidate for drug delivery systems.

DS Releasing. The DS was loaded onto the optimized silver/salep-g-PAA HN sample and its release was studied as a function of time. The release profile of DS from this loaded HN in pH 2 and pH 8 is shown in Figure 5. This Figure shows a negligible release of DS from loaded HN for first 5 h at pH 2. The DS remains within the HN due to its shrunken structure in acidic media. After 5 h, this DS loaded HN was transferred into pH 8. In pH 8, the HN swelled and showed higher release rate of DS as compared to pH 2. A sustained release of DS was observed for 6 h in pH 8. The release behavior of DS at different pHs is in good agreement with the swelling response of silver/salep-g-PAA HN at different pHs as previously discussed. To sum up, entitled hydrogel matrix can safely transfer the drug trough stomach with acidic pH and release it successfully in basic environment of colon, where the drug performance is good.

Characterization. In order to characterize the obtained hydrogel, we have recorded the FT-IR spectra of the hydrogels. The FT-IR spectra of salep-g-PAA, silver/salep-g-PAA HN, salep, and PAA are shown in Figure 6. The salep-g-PAA (Figure 6(a)) has shown absorption peaks at 1630 cm^{-1} and 1575 cm^{-1} relating to C=O stretching vibrations of PAA (Figure 6(d)) and glucomannan repeating units (Figure 6(c)) from salep. The peak observed at 3300 cm^{-1} is due to the stretching vibrations of OH and COOH functional groups in the polymer networks. The silver/salep-g-PAA HN (Figure 6(b)) has shown all the above characteristic peaks with a slight shift to higher wavelengths. This shifting can be attributed to the formation of coordinating bonds between the silver nanoparticles and the electron rich groups (such as C=O and OH) present in the hydrogel network.

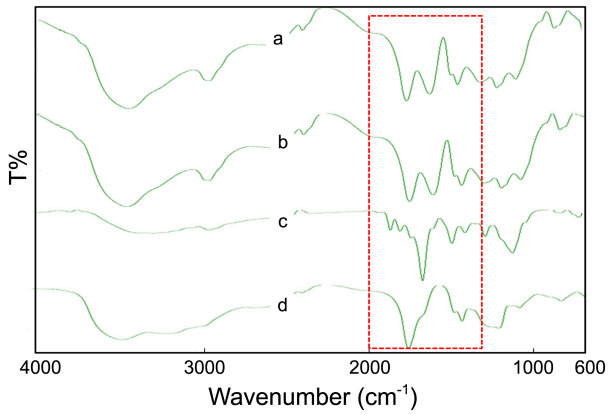

Figure 6. FT-IR spectra of (a) salep-g-PAA, (b) silver/salep-g-PAA HN, (c) salep, and (d) PAA.

The TGA analysis was applied to confirm the presence of silver nanoparticles in silver/salep-g-PAA HN structure. Figure 7 shows the percentage decomposition of salep-g-PAA and silver/salep-g-PAA HN. The salep-g-PAA had two main decomposition steps and near 95% of the salep-g-PAA had decomposed at 700 °C. However, two degradation steps with 80% weight loss at 700 °C were occurred in the case of silver/salep-g-PAA HN. The difference in decomposition between the salep-g-PAA and silver/salep-g-PAA HN was found about 11%. The presence of silver nanoparticles in the hydrogel networks can catalyze CO_2 elimination from polymer chains and accelerate the degradation process. Also, The first derivative of the TGA curve (DTG) shows that the maximum decomposition rate of the salep-g-PAA was occured in the broad peak at 301.5 ºC, while the maximum decomposition rate of the silver/salep-g-PAA HN was occured *via* a sharp peak at 504.8 ºC. According to DTA, at aforementioned temperatures for these samples, endothermic reactions cause their decompositions.

The surface structures of the salep-g-PAA and silver/salep-g-PAA HN samples were observed using SEM (Figure 8). The images of salep-g-PAA and silver/salep-g-PAA HN samples showed a porous structure which is the characteristic of hydrogel networks. The more clear images from

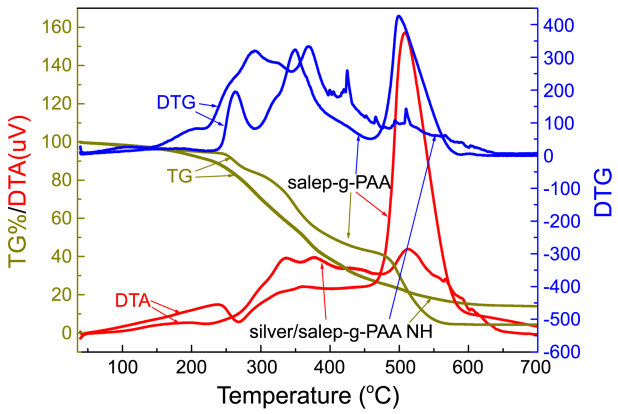

Figure 7. TGA/DTG/DTA curves of salep-g-PAA and silver/salep-g-PAA HN.

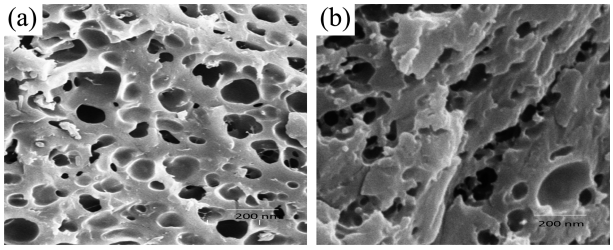

Figure 8. SEM images of (a) salep-g-PAA, and (b) silver/salep-g-PAA NH.

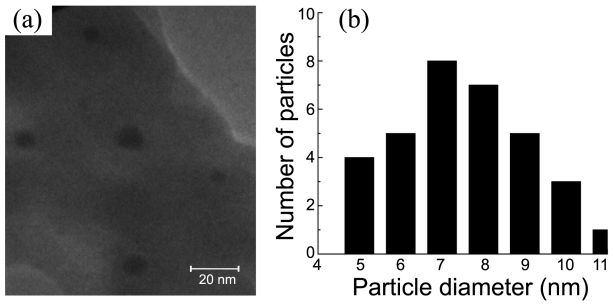

Figure 9. (a) TEM image and (b) the particle size histogram of silver/salep-g-PAA HN.

SEM to prove the presence of silver nanoparticles in the polymer matrix was failed. TEM images (Figure 9) was utilized for more precise study of the presence of silver nanoparticles in the silver/salep-g-PAA HN structure. The TEM image showed a highly uniform distribution of silver nanoparticles in the biopolymer matrix. It was confirmed that the silver nanoparticles in the cross-linked networks were spherical and highly dispersed in the biopolymer matrix with an approximate size of 5-10 nm.

Dynamic light scattering (DLS) has been also used to assess the diameters of the nanoparticles. The DLS data of silver/salep nanocomposite is shown in Figure 10. As one can see, the diameter of silver nanoparticles is between 5 to 10 nm which is in good agreement with the TEM data UV-vis absorption spectra of pure salep and silver/salep nanocomposite in water are demonstrated in Figure 11. In contrast to pure salep, the silver/salep nanocomposite exhibit a

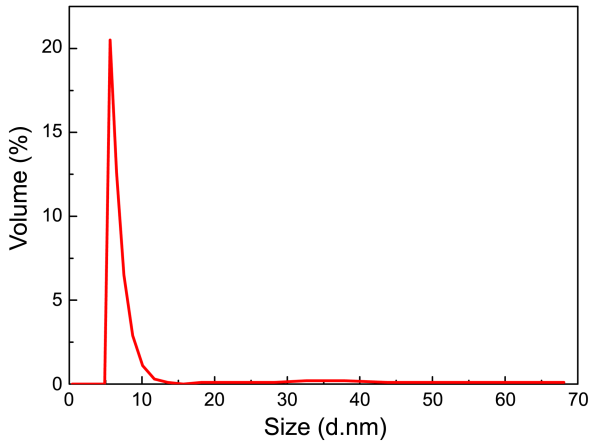

Figure 10. DLS data of silver/salep nanocomposite.

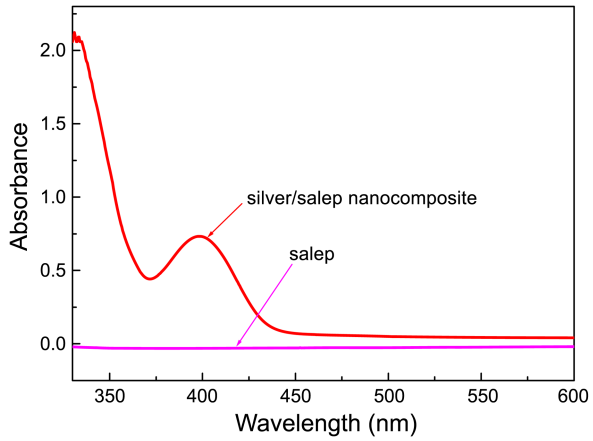

Figure 11. UV-vis absorption spectra of salep and silver/salep nanocomposite in water.

sharp peak between 385 and 410 nm (Figure 11). This peak is assigned to surface plasmon resonance absorption of the electrons in the conducting silver bands.[10] When a dielectric polymer-metal nanocomposite is excited by light, photons are coupled at the dielectric polymer-metal interface, causing an induced charge density oscillation that creates a strong absorption peak at a particular wavelength.

Conclusions

The silver/salep-g-PAA HN based on natural salep as a biopolymer backbone was prepared by a graft copolymerization reaction. The structural analysis of the silver/salep-g-PAA HN by FTIR confirmed the presence of the feed components in the nanocomposite. The silver/salep-g-PAA HN showed higher thermal stability than salep-g-PAA which confirmed the presence of silver nanoparticles in HN. The TEM images showed that the silver nanoparticles with average particle size of 5-10 nm are almost dispersed uniformly in the biopolymer based hydrogel. Modifying AA and silver ion can greatly improve the swelling of corresponding silver HN. The response of the prepared nanocomposite against pH made this silver/salep-g-PAA HN suitable for the release of DS in simulated colon environment. The more experiments regarding to the antibacterial activity of this HN is under investigation and we will report the results in near future.

Acknowledgments. We are grateful to the PNU for funding this work.

References

1. Mahdavinia, G. R.; Marandi, G. B.; Pourjavadi, A.; Kiani, G. *J. App. Poly. Sci*. **2010**, *118*, 2989.
2. Zhou, C.; Wu, Q. *Colloids Surf. B* **2011**, *84*, 155.
3. Zhang, Y. T.; Fan, L. H.; Zhi, T. T.; Zhang, L.; Huang, H.; Chen, H. L. *Polymer* **2009**, *50*, 5693.
4. Wang, Y.; Chen, D. *J. Colloid Interface Sci.* **2012**, *372*, 245.
5. Galvez, N.; Fernández, B.; Sánchez, P.; Morales-Sanfrutos, J.; Santoyo-González, F.; Cuesta, R.; Bermejo, R.; Clemente-León,

M.; Coronado, E.; Soriano-Portillo, A.; Domínguez-Vera, J. M. *Solid State Sci.* **2009**, *11*, 754.
6. Yallapu, M. M.; Othman, S. F.; Curtis, E. T.; Gupta, B. K.; Jaggi, M.; Chauhan, S. C. *Biomaterials* **2011**, *32*, 1890.
7. Veerasamy, R.; Xin, T. Z.; Gunasagaran, S.; Xiang, T. F. W.; Yang, E. F. C.; Jeyakumar, N.; Dhanaraj, S. A. *J. Saudi Chem. Soc.* **2011**, *15*, 113.
8. Murthy, P. S. K.; Mohan, Y. M.; Varaprasada, K.; Sreedhar, B.; Raju, K. M. *J. Colloid. Interface Sci.* **2008**, *318*, 217.
9. Thomas, V.; Yallapu, M. M.; Sreedhar, B.; Bajpai, S. K. *J. Colloid Interface Sci.* **2007**, *315*, 389.
10. Vimala, K.; Sivudu, K. S.; Mohan, Y. M.; Sreedhar, B.; Raju, K. M. *Carbohydr. Polym.* **2009**, *75*, 463.
11. Mohan, Y. M; Vimala, K.; Thomas, V.; Varaprasad, K.; Sreedhar, B.; Bajpai, S. K.; Raju, K. M. *J. Colloid Interface Sci.* **2010**, *342*, 73.
12. Zhou, N. I.; Liu, Y.; Li, L.; Meng, N.; Huang, Y. X.; Zhang, J.; Wei, S. H.; Shen, J. *Curr. Appl. Phys.* **2007**, *7S1*, e58.
13. Luo, Y. L.; Wei, Q. B.; Xu, F.; Chen, Y. S.; Fan, L. H.; Zhang, C. H. *Mater. Chem. Phys.* **2009**, *118*, 329.
14. Jovanovi, Z.; Stojkovska, J.; Obradovi, B.; Miskovic-Stankovi, V. *Mater. Chem. Phys.* **2012**, *133*, 182.
15. Huang, X.; Xiao, Y.; Zhang, W.; Lang, M. *Appl. Surface Sci.* **2012**, *258*, 2655.
16. Tolaymat, T. M.; Badawy, A. M. E.; Genaidy, A.; Scheckel, K. G.; Luxton, T. P.; Suidan, M. *Sci. Total Environ.* **2010**, *408*, 999.
17. Pourjavadi, A.; Soleyman, R.; Bardajee, G. R. *Starch-Starke* **2008**, *60*, 468.
18. Farhoosh, R.; Riazi, A. *Food Hydrocolloids* **2007**, *21*, 660.
19. Roberts, M. C. *FEMS Microbiol. Rev.* **1996**, *19*, 1.
20. Francisa, S.; Kumar, M.; Varshneya, L. *Radiat. Phys. Chem.* **2004**, *69*, 481.
21. Chena, J.; Liua, M.; Chena, S. *Mater. Chem. Phys.* **2009**, *115*, 339.